

Rheological, Thermal, and Morphological Characteristics of Plasticized Cellulose Acetate Composite with Natural Fibers

Joon Soon Choi,¹ Sung Taek Lim,¹ Hyoung Jin Choi,*¹ Soon Man Hong,² Amar K. Mohanty,³ Lawrence T. Drzal,⁴ Manjusri Misra,⁴ Arief C. Wibowo⁴

¹Department of Polymer Science and Engineering, Inha University, Incheon, 402-751, Korea

E-mail: hjchoi@inha.ac.kr

²Polymer Hybrid Center, Korea Institute of Science and Technology, Seoul 136-791, Korea

³The School of Packaging, 130 Packaging Building, Michigan State University, East Lansing, MI 48824, USA

⁴Composite Materials and Structures Center, Department of Chemical Engineering and Materials Science, Michigan State University, MI 48824, USA

Summary: Plasticized cellulose acetates processed with biofibers like industrial hemp and henequen were investigated with respect to their thermal, morphological and rheological characteristics. Discernable fibril morphologies in the biocomposites were observed via a SEM investigation. Such morphological characteristics were further analyzed with the results of TGA and rheometry. Furthermore, the obtained rheological properties were also interpreted in conjunction with the formation and destruction of internal structure in biocomposites.

Keywords: biocomposite; biodegradable; biofiber; cellulose acetate; rheology

Introduction

In addition to a growing need to develop novel bio-based products and other innovative technologies that can resolve widespread dependence on fossil fuel, sustainability, industrial ecology, eco-efficiency, and green chemistry are guiding the development of the next generation of materials, products, and processes. Thus, it places biodegradable polymers and bio-based polymers in an important position due to their potential to protect the environment by reducing plastic waste pollution and to be used as renewable resources for polymer manufacturing.^[1] These include poly(hydroxybutyrate)^[2,3], poly(ϵ -caprolactone) (PCL) and polylactide (PLLA)^[4,5], biodegradable aliphatic polyesters (BAPs)^[6] and bio-based materials such as wood, wood wastes and residues, grasses, crops and natural fibers.^[7-10] Among these biodegradable polymers or bio-based polymer

products, cellulose from trees is the most highly attractive as a substitute for petroleum feedstock in making plastics for the consumer market since it is strong, light weight, abundant, renewable, nonabrasive, and biodegradable.^[9] The molecular structure of cellulose provides a building block in plants because of the rigidity of the cellulosic chains, in which the rigidity originates from the hydrogen bonding of the free hydroxyl groups in the glucose repeating unit within and between chains. The stability of the superstructure that is formed (microfibrils and fibrils) comes mainly from the ability to form hydrogen bonds. As a consequence, cellulose is not a thermoplastic but degrades on heating before the theoretical melting point is reached. Breaking the hydrogen bonds by solubilizing and reacting the free hydroxyl groups yields a polymer that is thermoplastic. Cellulose plastics, such as cellulose acetate (CA), plasticized cellulose acetate (CAP), and cellulose acetate butyrate (CAB), are thermoplastic materials produced through the esterification of cellulose. A variety of raw materials such as cotton, recycled paper, wood cellulose, and sugar cane are used in making cellulose ester biopolymers in powder form. Such powders combined with plasticizers and additives are extruded to produce various grades of commercial cellulosic plastics in pelletized form.

On the other hand, as an effective way to improve the polymer properties, addition of the second component to the polymer matrix has been adopted in various fields, since it can hybridize the properties of the two components, representing superior physical and mechanical properties - such as solvent resistance, electrical characteristics, optical properties, heat resistance, and flammability - when compared with pristine commercial polymers.^[11-16]

In processing the polymer composite, biofibers such as henequene (HQ), kenaf, flax, jute, sisal, and industrial hemp (HP) can be successful candidates for reinforcing the strength and stiffness in the final composite. Compared to conventional fibers like glass, carbon, aramid, etc., these biofibers possess various considerable characteristic properties.^[17] This depends on whether the fibers are taken from plant stems or leaves^[18], the quality of the plant locations^[19], the age of the plant and preconditioning.^[20] Depending on their origin, the natural fibers may be grouped into leaf (henequen), bast (hemp), seed, and fruit origin. Considering both the eco-friendliness and superior material properties, biodegradable composites incorporated with natural fibers would give the most successful basis for next generation structural materials. Recent development in biodegradable polymer/clay nanocomposites is also noteworthy.^[21-23]

In this work, plasticized cellulose acetate (CAP) was melt-processed with two different types of biofibers: henequen and industrial hemp. Using these prepared samples, we investigated their characteristic thermal stabilities, fractured surface morphologies, and rheological properties in an oscillatory shear mode, fully taking into account the effects of different types of biofibers on the characteristics of biocomposites.

Most commercial cellulose acetate products are clear, strong and stiff, possessing a broad range of applications. Some applications of cellulose ester biopolymers are film substrates for photography, toothbrush handles, selective filtration membranes in medicine, and automotive coatings.^[24] Nonetheless, the main drawback of cellulose acetate is that its melt processing temperature is very close to its decomposition temperature, as determined by the structure of its parent cellulose. It implies that cellulose acetates should be plasticized prior to being used for thermoplastic processing applications.^[25] In this study, we used CAP containing 30 wt% of plasticizer as dispersing medium for biofibers.

Experimental

The main components of biofibers (lignocelluloses) are known to be cellulose, hemicellulose and lignin. Among these, cellulose is a hydrophilic glucan polymer consisting of a linear chain and containing hydroxyl groups. Therefore, all of the natural fibers are in general hydrophilic in nature. The details about these biofibers^[26] are summarized in Table 1.

To prepare biocomposites based on the natural fibers, a two-step extrusion process was carried out. In the first extrusion step, plasticized cellulose acetate (CAP) pellets were made by pre-mixing cellulose acetate (CA) (Eastman Chemical Co., Kingsport, TN, USA) powder with 30 wt% triethyl citrate (TEC) plasticizer (Morflex Inc., Greensboro, NC, USA). In the second step, CAP pellets, as obtained through the first process, were fed into the twin-screw extruder (ZSK-30 from Werner-Pfleiderer with L/D = 30 and six temperature controlled zone) while feeding the chopped natural fibers, either hemp or henequen, into the last zone of the extruder. The temperature profiles along the barrel were 190 °C with the die temperature held at 195 °C. A screw speed of 150 rpm was used with ~40% torque reading, and the resulting output was 65-70 g/min.

The prepared biocomposites were designated as CAP30, HPCAP30, and HQCAP30. Except CAP30 (plasticized cellulose acetate) itself, the first two letters stand for the fiber materials as follows: HQ (henequen) and HP (hemp). The last two digits of 30 means a

weight concentration of the plasticizer in CAP. Though it was not shown in the abbreviation of the sample names, the fiber content was fixed as 30 wt% in all cases. These samples were then compression molded into a disc type sample in a hot press (HP-200L, Kee-Pae, Seoul, Korea) at 210 °C under the pressure of 1,000 psi.

Table 1. Chemical composition and structural parameters of hemp and henequen.

	type	Cellulose (wt%)	lignin (wt%)	Hemicelulose (wt%)
Hemp	bast	70.2-74.4	3.7-5.7	17.9-22.4
Henequen	leaf	77.6	13.1	4-8

The fractured morphologies were examined using a scanning electron microscope (SEM, Hitach S-4300, Japan) with various magnifications at 15 kV. The surfaces were coated with platinum to generate electric current on the surfaces. Thermal stability was examined using a thermogravimetric analysis (TGA) (TA Instrument Q50, USA) from 30 to 650 °C, under a nitrogen atmosphere at a heating rate of 20 °C/min. Rheological properties of the samples were measured via a rotational rheometer with a parallel-plate geometry (Physica, MCR 300, Germany) of 1.1 mm thickness and 25 mm diameter at 210 °C. In an oscillatory shear mode, we examined the durability of the samples for vibration or periodic external stress. The storage modulus (G') and loss modulus (G'') were then measured as a function of frequency with a deformation of 0.01 % for the biocomposites except CAP30 (~1%).

Results and Discussion

Surface morphology obtained from the SEM is shown in Figure 1. In particular, Fig. 1(a) indicates the relatively smooth surface of a pristine matrix polymer (CAP30) at the magnification of 100. This surface characteristic was abruptly altered by the addition of biofibers of hemp and henequen, respectively (Fig. 1(b) and 1(c)). The investigation of a fractured surface can be used as an effective method to verify the role of biofibers in the composites. For this purpose, we added the images of bare biofibers for corresponding composites (insets) into the fractured images of biocomposites. When compared with those of the bare fibers given in Fig. 1(b) and 1(c), it is not difficult to conclude that the final morphologies of the biocomposites are decided by the fibers. As described above, the

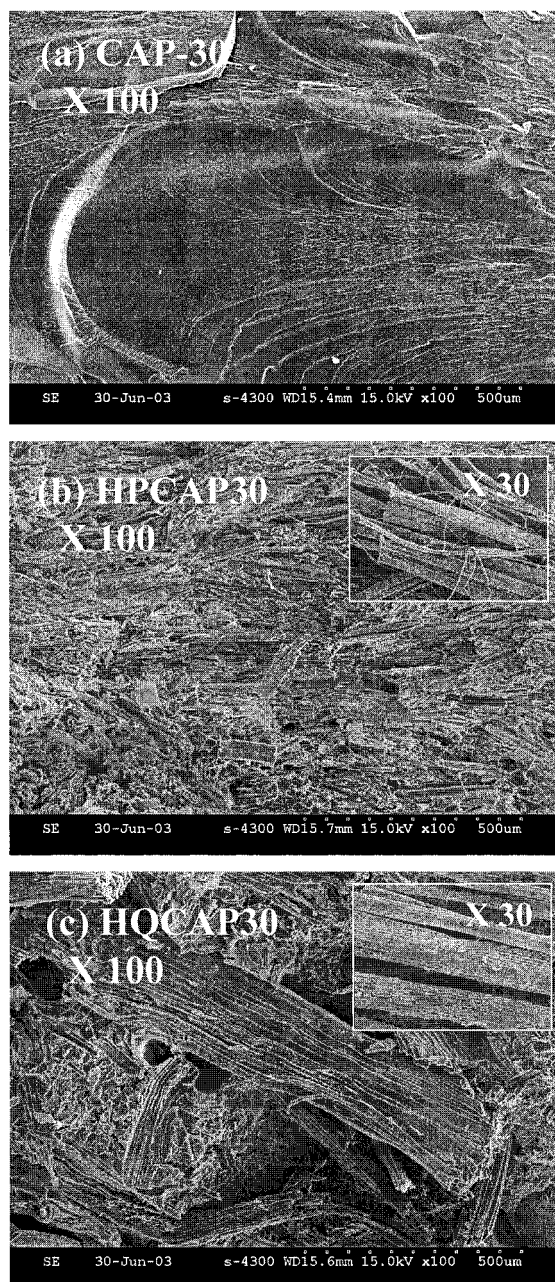


Figure 1. Scanning electron micrographs (SEM) of (a) CAP30, (b) HPCAP30, and (c) HQCAP30 at the magnification of 100. The insets show the pristine fibers for each system ($\times 30$).

fiber content (30 wt%) was too high to accomplish the homogeneous internal state. In addition, the original structures and morphology of biofibers are maintained in the biocomposite without any deterioration. This means that other final characteristics would be mainly governed by the biofiber itself, not by the matrix polymer. In the case of Fig. 1(b) for the HPCAP30 and Fig. 1(c) for the HQCAP30, it is not easy to distinguish the matrix polymer from fiber morphology. In other words, it may be possible that the matrix polymer plays a role to wet or bind the major robust biofibers.^[27]

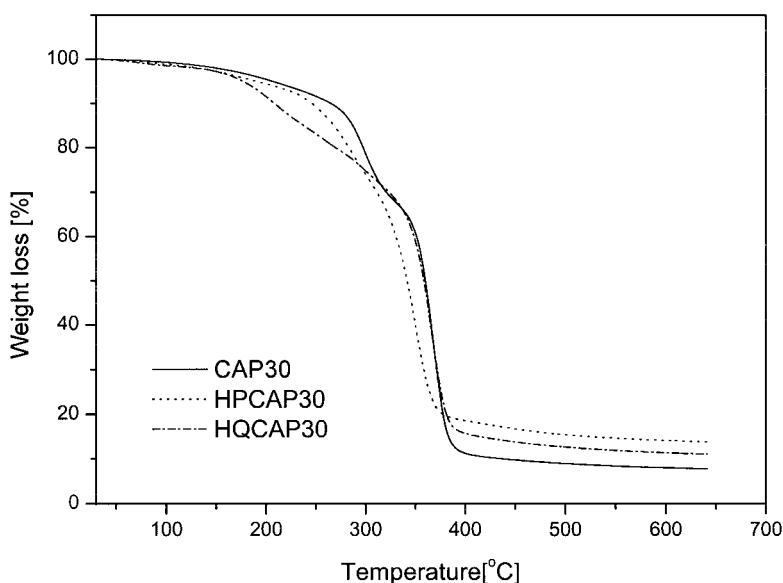


Figure 2. Thermogravimetric analysis of CAP30, HPCAP30, and HQCAP30. The temperature scanning speed was set as 20 °C/min under N₂ surrounding.

Figure 2 represents the TGA curves of pure plasticized cellulose (CAP30) and its biocomposites. As indicated in the previous study,^[25] CAP30 exhibits the characteristic two-step decomposition behavior caused by the addition of plasticizer. In the cases of HPCAP30 and HQCAP30, three major transitions from those of CAP30 can be addressed. First, a two-step process in the CAP30 changed into a quasi single-step process. It was already suggested indirectly from the SEM investigation based on the plasticizer content. As described above, the biofiber, which governed the surface morphologies, also

determined the decomposition process. It can be conjectured that the wetted matrix resin in the fiber could not display its characteristic two-step process. Second, inferior thermal stability of biofibers triggered the early stage decomposition. Finally, the residual weight of the biocomposite is somewhat higher than that of the CAP30. Char formation of about 10% for the CAP30 increased with the addition of biofibers. Namely, the residual weight of biofibers was observed to be about 20–30%, implying that the increase of the residual weight of the biocomposite might be generated by fibers.

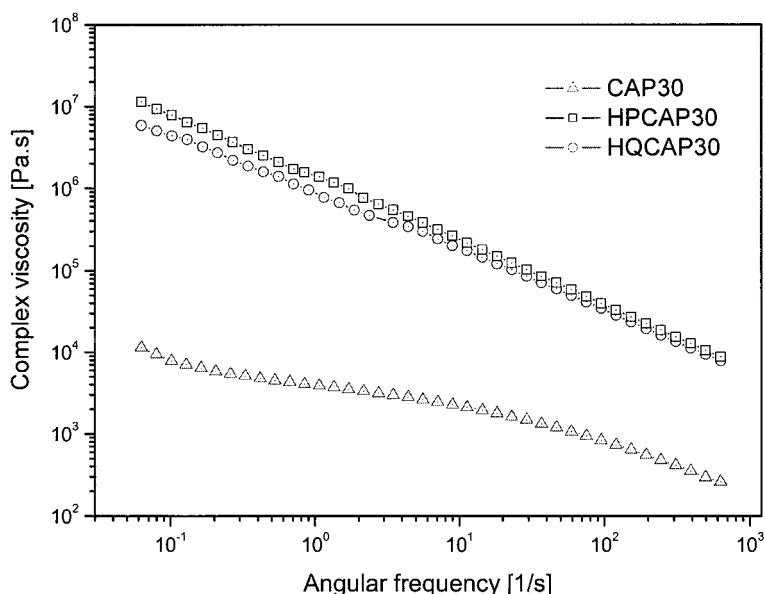


Figure 3. Complex viscosities vs. angular frequency for CAP30, HPCAP30, and HQCAP30 measured at 210 °C.

Measured rheological properties of both complex viscosity and dynamic moduli at 210 °C are plotted as a function of angular frequency for CAP30 and its biocomposites, as given in Fig. 3 and 4, respectively. Since the thermal decomposition starts at around 200 °C, rheological measurements performed at 210 °C might be affected; however, the effect is negligible. From these oscillatory measurements, we can investigate the viscoelastic responses of the materials without any destruction of the internal structure of the samples, since the experimental test was performed within a linear viscoelastic region.^[28, 29] That is,

prior to the test of sweeping the angular frequency, a pre-test was performed to verify the linear correlation between amplitude and material function, such as the storage or loss modulus. At a fixed temperature, these values are only the function of frequency. This means that the storage and loss modulus obtained as a function of applied strain should be a constant at a fixed frequency in a linear viscoelastic region. The deviation of such linearity implies the destruction of internal structure. As a result, the examination of a linear region has two important meanings: one is the validity of viscoelastic properties and the other is the order of magnitude for the linearity, which effectively represents the material characteristics. Except CAP30, the pre-set amplitude for the oscillatory measurement was chosen as 0.01%, which was abnormally smaller than that of usual polymer melt, indicating that the fluidity of the composite was very different from that of CAP30. In the case of CAP30, the amplitude for the dynamic measurement was fixed at 1%.

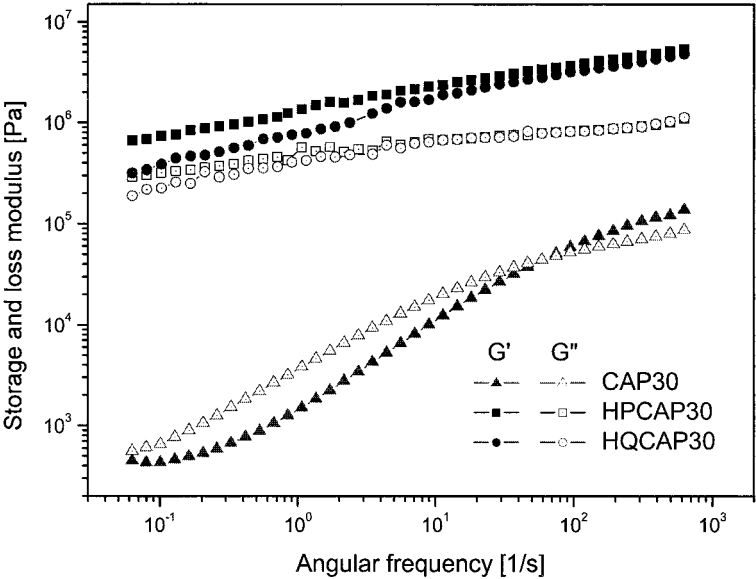


Figure 4. Storage (filled symbols) and loss (open symbols) modulus of CAP30, HPCAP30, and HQCAP30 measured at 210 °C.

In Fig. 3, the complex viscosities of biocomposites were found to be much higher than that of CAP30 by two orders of magnitude at least. Moreover, the degree of shear thinning for biocomposites is much enhanced by the addition of biofibers. This can be explained by the alignment of added fiber in the matrix polymer. The induced shear flow makes each fibril component be aligned in the direction of flow. This alignment reduced the flow resistance, resulting in the gradual decrease of complex viscosities. When we compared these results with both SEM and TGA investigations, we could also find some consistent features. As described in the analysis of Fig. 1, the flow behavior of HPCAP30 and HQCAP30, in which we could not find a discernable matrix polymer portion, was governed by the fiber itself, as anticipated in the SEM analysis.

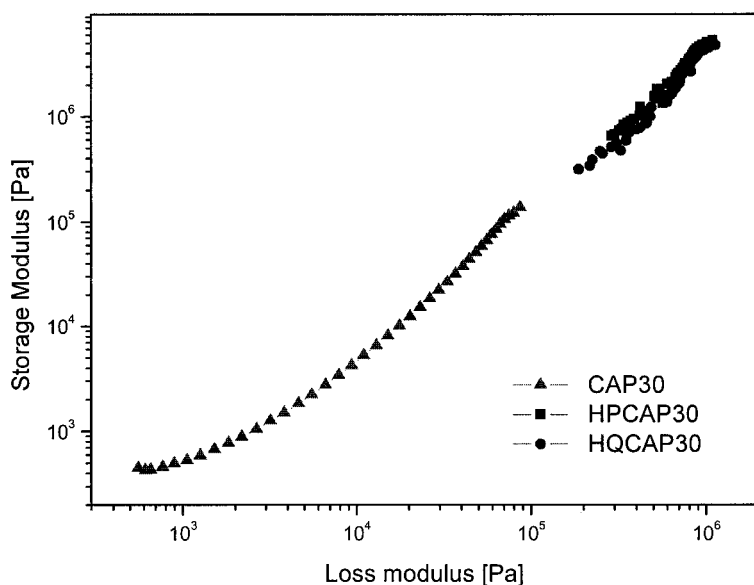


Figure 5. Modified Cole-Cole plot (G' vs G'') for CAP30, HPCAP30, and HQCAP30 at 210 °C.

From this oscillatory test mode in the rheological measurements, in addition to the complex viscosity, we can also get storage (G') and loss (G'') moduli as a function of angular frequency. Compared to the CAP30, the addition of biofibers showed the remarkable increase in both G' and G'' . In addition, a transition of the slopes to a flattened

behavior with biofibers, i.e., non-terminal behavior, was observed at relatively low frequencies. Thereby, the low frequency response can be regarded as a solid-like behavior caused by fibril components. The melt behavior of the CAP30 is liquid-like ($G' < G''$) at low frequencies while solid-like behavior ($G' > G''$) is found at high frequencies.^[30] The crossover frequency ω_c is defined as $G'(\omega_c) = G''(\omega_c)$. However, ω_c cannot be indistinguishable between HPCAP30 and HQCAP30. For the entire frequency range, both decreased frequency dependency and a much higher storage modulus were observed. It was also found that the overall viscoelastic behavior exhibited a solid-like one, and was mainly governed by the addition of biofibers.

A modified Cole-Cole plot, a logarithmic plot of G' against G'' for CAP30, HPCAP30, and HQCAP, is represented in Figure 5. Although as yet there exists no fundamental theoretical background available to explain its mechanism fully, it is well-known that a modified Cole-Cole plot gives a master curve with a slope of 2 for homogeneous polymer melts and solutions.^[31,32] Therefore, we can expect that all the samples should give a master curve with a slope of 2, if the samples are homogeneous. However, the samples give a curve with a slope less than 2, due to the heterogeneity of the samples by the addition of plasticizer and biofiber. Furthermore, a logarithmic plot of G' against G'' for biocomposites is independent of the biofibers used in this study. Thus, we can conclude that morphologies for both biocomposites are very similar.^[33] This agrees with the results in the oscillation test that the overall viscoelastic behavior is mainly governed by the addition of biofibers.

Conclusion

We investigated thermal, morphological and rheological characteristics of the plasticized cellulose acetate (CAP) processed with two different biofibers of hemp and henequen. Via a SEM investigation, discernable fibril morphologies in the composites were observed. Such morphological characteristics were further analyzed with the results of TGA and rheometry. We found that the two-step decomposition process of plasticized CAP30 was apparently affected by the addition of biofibers. In addition, obtained rheological properties of the complex viscosity, dynamic moduli and a modified Cole-Cole plot were interpreted in conjunction with the formation and destruction of the internal structure in the biocomposites. With the addition of biofibers, we also observed large increases of

complex viscosity, storage modulus and loss modulus, along with a solid-like behavior over a wide range of frequency.

Acknowledgement

This study was partially supported by research grants from the Industrial Waste Recycling R&D Center, Korea. Partial financial support from the NSF/EPA (Award Number DMI-0124789) under the 2001 Technology for a Sustainable Environment (TSE) program is gratefully acknowledged. The authors also thank Eastman Chemical Company (Kingsport, TN, USA) for the cellulose ester samples, Flaxcraft, Inc. (Cresskill, NJ, USA), for supplying natural fibers and Morflex, Inc. (Greensboro, NC, USA), for supplying citrate plasticizer.

- [1] Y. Ikada, H. Tsuji, *Macromol. Rapid Commun.* **2000**, *21*, 117.
- [2] H. J. Choi, S. H. Park, J. S. Yoon, H. S. Lee, S. J. Choi, *Polym. Eng. Sci.* **1995**, *35*, 1636.
- [3] S. H. Park, H. J. Choi, S. T. Lim, T. K. Shin, M. S. Jhon, *Polymer* **2001**, *42*, 5737.
- [4] J. J. Cooper-White, M. E. Mackay, *J. Polym. Sci. Polym. Phys.* **1999**, *37*, 1803.
- [5] E. S. Park, H. K. Kim, J. H. Shim, H. S. Kim, J. W. Jang, J. S. Yoon, *J. Appl. Polym. Sci.* **2004**, *96*, 3508.
- [6] J. Kim, S. T. Lim, H. J. Choi, M. S. Jhon, *Macromol. Chem. Phys.* **2001**, *202*, 2634.
- [7] G. Toriz, R. Arvidsson, M. Westin, P. Gatenholm, *J. Appl. Polym. Sci.* **2003**, *88*, 337.
- [8] V. Tserki, P. Matzinos, C. Pangyiotou, *J. Appl. Polym. Sci.* **2003**, *88*, 1825.
- [9] W. Liu, A. K. Mohanty, L. T. Drzal, P. Askel, M. Misra, *J. Mater. Sci.* **2004**, *39*, 1051.
- [10] G. Mehta, A. K. Mohanty, M. Misra, L. T. Drzal, *J. Mater. Sci.* **2004**, *39*, 2961.
- [11] Y. Kojima, A. Usuki, A. Okada, T. Kurauchi, O. Kamigato, *J. Mater. Res.* **1993**, *8*, 1174.
- [12] J. W. Gilman, *Appl. Clay Sci.* **1999**, *15*, 31.
- [13] R. A. Vaia, K. D. Jandt, E. J. Kramer, E. P. Giannelis, *Macromolecules* **1995**, *28*, 8080.
- [14] J. W. Kim, F. Liu, H. J. Choi, *J. Ind. Eng. Chem.* **2002**, *8*, 399.
- [15] R. A. Vaia, E. P. Giannelis, *Macromolecules* **1997**, *30*, 7990.
- [16] G. S. Sur, S. G. Lyu, J. H. Chang, *J. Ind. Eng. Chem.* **2003**, *9*, 58.
- [17] A. K. Bledzki, S. Reihmane, J. Gassan, *J. Appl. Polym. Sci.* **1996**, *59*, 1329.
- [18] E. T. N. Bisanda, M. P. Ansell, *J. Mater. Sci.* **1992**, *27*, 1690.
- [19] B. C. Barkakaty, *J. Appl. Polym. Sci.* **1976**, *20*, 2921.
- [20] P. K. Ray, A. C. Chakravarty, S. B. Bandyopadhy, *J. Appl. Polym. Sci.* **1976**, *20*, 1765.
- [21] Y. H. Hyun, S. T. Lim, H. J. Choi, M. S. Jhon, *Macromolecules* **2001**, *34*, 8084.
- [22] S. T. Lim, Y. H. Hyun, H. J. Choi, M. S. Jhon, *Chem. Mater.* **2002**, *14*, 1839.
- [23] S. T. Lim, C. H. Lee, H. J. Choi, M. S. Jhon, *J. Polym. Sci. B : Poly. Phys.* **2003**, *41*, 2052.
- [24] K. J. Edgar, C. M. Buchanan, J. S. Debenham, P. A. Rrndquist, B. D. Seller, M. S. Shelton, D. Tindal, *Prog. Polym. Sci.* **2001**, *26*, 1607.
- [25] A. K. Mohanty, A. Wibowo, M. Misra, L. T. Drzal, *Polym. Eng. Sci.* **2003**, *43*, 1151.
- [26] A. K. Mohanty, M. Misra, G. Hinrichsen, *Macromol. Mater. Eng.* **2000**, *276/277*, 1.
- [27] C. Baley, Y. Grohens, F. Busnel, P. Davies, *Appl. Compos. Mater.* **2004**, *11*, 77.
- [28] S. H. Park, S. T. Lim, T. K. Shin, H. J. Choi, M. S. Jhon, *Polymer* **2001**, *42*, 5737.
- [29] Z. Y. Zhu, P. Dakwa, P. Tapadia, R. S. Whitehouse, S. Q. Wang, *Macromolecules* **2003**, *36*, 4891.
- [30] H. J. Choi, S. G. Kim, Y. H. Hyun, M. S. Jhon, *Macromol. Rapid Commun.* **2001**, *22*, 320.
- [31] C. D. Han, M. S. Jhon, *J. Appl. Polym. Sci.* **1986**, *32*, 3809.
- [32] H. J. Choi, J. H. Kim, J. Kim, S. H. Park, *Macromol. Symp.* **1997**, *119*, 149.
- [33] H. J. Choi, J. Kim, M. S. Jhon, *Polymer* **1999**, *40*, 4135.

